PORTATION

UNIVERSITY OF MINNESOTA

TESTING OF SOIL HEAT AND WATER FLOW MODELS

Xia Xu and John Nieber,
Agricultural Engineering;
John M. Baker, Soil Science;
David E. Newcomb,
Civil and Mineral Engineering

Sponsored by:
Center for Transportation Studies

The financial support of oil overcharge funds distributed through the Minnesota Department of Administration is acknowledged, but the authors assume complete responsibility for the contents herein.

TESTING OF SOIL HEAT AND WATER FLOW MODELS

Xia Xu
Graduate Research Assistant
John L. Nieber
Associate Professor
Department of Agricultural Engineering
John M. Baker
Assistant Professor
USDA-ARS
Soil Science Department
and
David E. Newcomb
Assistant Professor
Civil and Mineral Engineering Department
University of Minnesota

ABSTRACT

The SHAW model (Simultaneous Heat And Water) is tested with water content and temperature profile data for a soil located near Rosemount Minnesota. The predicted frost/thaw depth, soil water content, and temperature at depths of 10, 20, 40, 80, and 100 cm are compared to measured values. The results show that the prediction of frost depth and temperature profile agree well with measured field data, while agreement between measured and predicted liquid water content is not as good.

INTRODUCTION

Seasonal freezing and thawing of soil occurs in a large part of the earth's land mass. Freezing/thawing phenomenon affect many natural processes and have a significant influence on many of man's activities An extensive review of current knowledge on frozen soils was prepared by Lundin (1989). Another review of current understanding of the processes associated with heat and mass transfer in freezing soils was presented by Kay and Perfect (1988).

Lundin (1989) reported that the freezing/thawing process improves the structure of many heavy clays soils and thereby increases the cultivation potential of these soils.

However, in other soils, the freezing/thawing process may degrade the soil structure. This suggests that freezing and thawing increases aggregation in undisturbed soils but may decrease aggregation in the cultivated soils.

Because the freezing/thawing process greatly influences the partitioning between infiltration and runoff of snowmelt and rainfall (Lundin, 1989) it has a major impact on runoff generation and soil erosion (Pikul and Allmaras, 1984; Flerchinger and Saxton, 1989). The process also influences the redistribution of soil water (Jumikis, 1958; Palmer, 1967)during the winter months and will thereby affect the magnitude and temporal distribution of groundwater recharge.

Due to its influence on soil water redistribution during winter months the freezing/thawing process impacts the fate of solutes present in the soil profile. Miller(1980) has reported the upward redistribution of solutes toward the frozen zone of the soil profile during freezing periods.

The problems associated with road construction on seasonally and permanently frozen soil are common (Wallace and Williams, 1974; Berg et al., 1980). The process of soil freezing can dramatically increase the mechanical strength of the soil and the ability of the soil to transmit water(Miller,1980). In contrast the thawing process of the soil can dramatically decrease the mechanical strength of the soil.

The modeling of heat and water transport in frozen soil can improve our understanding of the physics of a particular process and/or to predict the outcome of that process for certain boundary conditions (Kay and Perfect, 1988). Significant advances have been made in the past decade in understanding of processes which contribute to the movement of heat and mass in soils when freezing occurs. These advances have been facilitated by the introduction of new technology for measuring critical variables and parameters. There has also been considerable progress in integrating the description of these processes in models which are capable of accurately predicting heat and mass transport under an increasing range of conditions (Kay and Perfect, 1988).

The objectives of the study reported in this paper are: 1). to test and evaluate the heat and water flow model (SHAW model) with measured field data; and 2). to evaluate the sensitivity of heat and water transport in variably-saturated, variably-frozen soil to soil hydraulic and thermal properties.

GOVERNING EQUATIONS

Conservation Laws

Mass

Assuming the compressibility of the porous medium (here it is soil) and of the fluid (here it is water) is negligible compared to the change in saturation of the porous medium, which is true for natural flow conditions, the conservation of mass for fluid flow can be expressed in the form,

$$\frac{\partial(\rho_w \theta)}{\partial t} = -\nabla \cdot (\rho_w q_w) \pm S_w(x,t) \qquad (1)$$

where ρ_w = density of water, kg/m^3;

θ = volumatric water fraction, m^3/m^3;

t = time, sec;

$q_w = q_{wx} i + q_{wy} j + q_{wz} k$ (q_{wx}, q_{wy}, and q_{wz} are water fluxes in the x, y, and z directions, respectively), kg / m sec;

S_w = source / sink term, $kg/m^3 sec$;

Equation (1) states that the rate of change of storage of fluid mass in the control volume is equal to the net inflow through the boundaries of the control volume, plus a source/sink term.

Heat

The equation for conservation of heat energy in soil can be expressed as,

$$\rho_m c_m \frac{\partial T}{\partial t} = -\nabla \cdot (q_h) \pm S_h(x,t) \qquad (2)$$

where ρ_m = mass density of the soil, kg/m^3;

c_m = specific heat capacity of the soil, w / m °C;

T = temperature, °C;

q_h = vector flux of heat, w/m^2 sec;

S_h = the heat source / sink term, w/m^3 sec;

Equation (2) states that the time rate of change in heat content of a volume element of the porous medium must equal the net inflow of heat through the boundaries of the control volume, plus the heat source/sink term.

Constitution Relations for the Flux Terms

The flow of water including water vapor and heat in the soil of natural field condition is driven by both the hydraulic gradient and the temperature gradient. The temperature gradient affects the water potential gradient and induce both water and vapor flow. The flowing liquid water and water vapor carry heat and affects the temperature gradient, reciprocally. Therefore, the interactive relation between water flow and heat flow leads to the simultaneous flow of heat and water. Hillel(1980) has categorized previous studies on the simultaneous heat and water flow into two different approaches, the mechanistic approach and the thermodynamic approach. These two approaches will be reviewed briefly in the following.

Mechanistic approach

The mechanistic approach is based on the concept of viscous flow of liquid water under the influence of gravity and of capillary and adsorptive forces, and on the concept of vapor movement by diffusion. The theory been presented by Philip and de Vries (1957), and Jury (1973). The water flux under combined water potential and temperature gradients in the soil can be expressed by

$$q_w / \rho_w = -D_T \nabla T - D_\theta \nabla \theta_w - k i \qquad (3)$$

where

$$D_T = D_{Tliq} + D_{Tvap} \qquad (4)$$

$$D_\theta = D_{\theta liq} + D_{\theta vap} \qquad (5)$$

D_T = thermal water diffusivity (two components, liquid part and vapor part), $m^2 / sec\ ^\circ C$;

D_θ = isothemal water diffusivity (two components, liquid part and vapor part), m^2 / sec;

k = the unsaturated hydraulic conductivity of the soil, m / sec;

i = unit space vector.

for the heat flux, after dropping terms of negligible importance (Philip and de Vries 1957; Jury, 1973), the mathematic formulation can by written as

$$q_h = -\lambda \, \nabla T - L_v D_{\theta vap} \nabla \theta_w \qquad (6)$$

where q_h = total heat flux, w / sec;

λ = apparent thermal conductivity of the soil, w / sec;

L_v = latent heat of vaporization of water, w / m^2;

$D_{\theta vap}$ = water vapor diffusivity under water potential gradient, m^2 / sec;

Substituting equation (3) and (6) into (1) and (2) respectively, the final coupled water and heat equations are given by equations (7) and (8) (Philip and de Vries, 1957).

$$\frac{\partial \theta_w}{\partial t} = \nabla \cdot (D_T \cdot \nabla T) + \nabla \cdot (D_\theta \cdot \nabla \theta_w) + \frac{\partial k}{\partial z} \qquad (7)$$

$$c_m \rho_m \frac{\partial T}{\partial t} = \nabla \cdot (\lambda \cdot \nabla T) - L_v \nabla \cdot \left(D_{\theta vap} \cdot \nabla \theta_w\right) \qquad (8)$$

Harlan (1973) used essentially the same theory and developed mass transport equations for flow in saturated or partially saturated heterogeneous porous medium subjected to freezing/thawing processes. The theory was based on an analogy between the mechanisms of water flow in variably-frozen soils and those in unsaturated soils. By use of this analogy a Darcian approach is applied to the analysis of fluid flow and a Fourier approach is applied to the analysis of heat transport. The resulting mathematical description given by Harlan for simultaneous fluid flow and heat transport in a variably-saturated, variably-frozen porous medium was composed of a system of four equations. Two equations described the constitutive relations for heat conduction and water flow, and the other two equations described the conservation of water and thermal energy.

Based on the mechanistic approach, Flerchinger (1987) and Flerchinger and Saxton (1989) developed the SHAW (Simultaneous Heat And Water) model for evaluating the effects of tillage and residue management on soil freezing. The SHAW model is a detailed physically-based model which predicts snowmelt, evaporation and profiles of temperature, soil water content, ice content, and solute concentration through the snow-residue-soil system.

The governing differential equations for the SHAW model(Flerchinger, 1987; Flerchinger and Saxton, 1989) are given by equations (9) and (10).

$$C\frac{\partial T}{\partial t}-\rho_i L_f\frac{\partial \theta_i}{\partial t}+L_v\left(\frac{\partial \rho_v}{\partial t}+\frac{\partial q_v}{\partial z}\right)=\frac{\partial}{\partial z}\left(\lambda\frac{\partial T}{\partial z}\right)-\rho_w c_w\frac{\partial (q_w T)}{\partial z}+S_h \qquad (9)$$

where C = volumatric heat capacity of soil, $w / m^{3\circ} C$;

ρ_i = density of ice, kg / m^3;

L_f = latent heat of fusion, J / kg;

θ_i = volumatric ice content, m / m;

ρ_v = vapor density in soil pore space, kg / m^3;

q_v = downward water vapor flux through soil, $kg / m\ sec$;

z = depth from soil surface, m;

c_w = specific heat capacity of water, $J / kg\ ^\circ C$.

$$\frac{\partial \theta_\ell}{\partial t}+\frac{\rho_i}{\rho_w}\frac{\partial \theta_i}{\partial t}=\frac{\partial}{\partial z}\left[k\left(\frac{\partial \psi_m}{\partial z}+1\right)\right]-\frac{1}{\rho_w}\frac{\partial q_v}{\partial z}+S_w \qquad (10)$$

where k = unsaturated hydraulic conductivity m / s;

ψ_m = soil matric potential, m.

These equations are derived on a differenital control volume and are similar to the one-dimensional form of equations (7) and (8). The major differences between these equations and the one-dimensional form of equations (7) and (8) are that the SHAW model equations include the phase change between liquid water and ice, the transport of heat by convection in the liquid phase, and source/sink terms for heat and soil water.

In equation (9), each term represents, respectively, specific stored due to a temperature increase; latent heat required to freeze water; latent heat of evaporation in the layer; net thermal conduction into the layer; net thermal advocation into the layer due to water flux; and a source/sink term (which may include solar and long-wave radiation). In equation (10), each term represents, respectively, the time rate change of volumetric liquid water content; the time rate change of volumetric ice content; net liquid flux into the layer; net vapor flux into a layer; and a source/sink.

For snowpack and residue, the water and heat equation are basically the same as equations (9) and (10), except that some terms are deleted due to the relative insignificance of the corresponding process(see Flerchinger,1987; Flerchinger and Saxton 1989 for detail).

The boundary conditions of heat for the soil are heat and vapor flux from the atmosphere, snow or residue above the soil and a specified temperature for lower boundary. For the water balance, the upper boundary conditions are vapor flux from the atmosphere, snow or residue above the soil and lower boundary condition is specified water content.

Thermodynamic approach

Taylor and Cary(1964) applied the theory of thermodynamics of irreversible processes and developed linear equations for the simultaneous flow of mass and transport of energy. The water and heat flow equations based on the thermodynamics of irreversible processes are expressed as functions of coupled water potential gradient and temperature gradient.

Kay and Groenevelt(1974) and Groenevelt and Kay(1974) used this approach for variably-frozen soils and derived system equations for water flow and heat transport, as well as the interrelationship of the transport coefficients. The equation for simultaneous moisture and heat movement can be written in matrix form as

$$\begin{bmatrix} q_v \\ q_w \\ q_h \end{bmatrix} = \begin{bmatrix} L_{vv} & L_{vh} \\ L_{ww} & L_{wh} \\ L_{hv} + L_{hw} & L_{hh} \end{bmatrix} \times \begin{bmatrix} -v_w \nabla \psi_h \\ -\nabla T / T \end{bmatrix} \tag{11}$$

where L_{vv}, L_{vh}, ... L_{hh} = transport coefficients, with subscripts

v = vapor,

w = liquid water,

h = heat;

v_w = specific volume of the liquid water, m^3/kg;

ψ_h = hydraulic pressure, pa.

In variably-saturated, variably-frozen soil where water vapor, liquid water, and ice occur simultaneously in equilibrium, the soil matric potential can be expressed as a function of vapor pressure of the ice phase, and vapor pressure of pure water (Hoekstra, 1966).

$$\psi_m = -\frac{RT}{v_w M} Ln\left(\frac{p_{ice}}{p_o}\right) \tag{12}$$

where ψ_m = matric potential;

R = gas constant, J / mol k;

M = molecular weight of water vapor, kg / mol;

p_{ice} = vapor pressure of ice phase;

p_o = vapor pressure of pure water.

The relationship between the temperature gradient and the hydraulic pressure gradient can be expressed by the Clapeyron equation (Groenevelt and Kay, 1974),

$$\nabla\psi_h = \left(\frac{H_f}{v_w}\right)\left(\frac{\nabla T}{T}\right) \tag{13}$$

where ψ_h = hydraulic pressure, pa;

H_f = specific latent heat of freezing, J / kg;

v_w = specific volume of the liquid water, m^3 / kg.

Based on the irreversible thermodynamics approach, Kung and Steenhuis (1986) developed a computer model to simulate water and heat flow in the soil under freezing conditions. The mathematical formulation of the coupled water and heat equations were expressed as a function of temperature (hydraulic pressure gradient has been incorporated in the temperature gradient) given by equation (14), (15), and (16) (Kung and Steenhuis, 1986).

$$q_v = \frac{MD_v \varepsilon\left(H_v + H_f\right)}{\tau R v_v T^2} \nabla(-T) \tag{14}$$

$$q_w = \left(K_s H_f / \eta v_w T\right)\nabla(-T) \tag{15}$$

$$q_h = \frac{H_v H_f}{H_v + H_f} q_v + \lambda\, \nabla(-T) \tag{16}$$

where D_v = diffusion coefficient of vapor in air, m^2 / s;

ε = air filled porosity, m^3 / m^3;

τ = tortuosity factor, m / m;

H_v = specific latent heat of vaporization, J / kg;

η = viscosity, Pa s;

Although the mechanistic and irreversible thermodynamics approaches are distinct in their individual formulations, they are somewhat similar in that they each describe the simultaneous flow and transport of heat in terms of coupled water potential and temperature gradients as seen in equations (3), (6), and (11). The main distinctions between the two approaches lies in the primary assumptions, the fundamental derivation of the equations, and the definition of the transport coefficients. Jury (1973) indicated that Philip and de Vries (1957) decomposed the simultaneous flux of heat and water into concentration and temperature parts. This is not done in the irreversible thermodynamics approach. Also Philip and de Vries (1957) concentrated the thermal dependence of driving forces in the temperature gradient term; the water content gradient term is essentially temperature independent. This is not true in the flux equations of irreversible thermodynamics approach (Jury, 1973).

Hillel (1980) suggested that the advantage of the irreversible thermodynamics is that it makes no a priori assumptions regarding the mechanisms of the transport phenomena formulated. With respect to the irreversible thermodynamics approach Hillel states "... it would seem to be less restrictive than a physical theory whose validity is constrained at the outset by its mechanistic assumptions. The disadvantage of the approach, however, is precisely in the failure to address itself to, and provide insight into, the nature and internal workings of the phenomena considered. For instance, it treats the phase change of water involved in the transfer of heat by vapor in an implicit way only".

Kung and Steenhuis (1986) and Kay and Perfect (1988) indicated that the theory of thermodynamics of irreversible processes is a promising approach to simulate water flow and heat transport in variably-saturated, variably-frozen soils. It should therefore be given additional serious consideration in future research on water flow and heat transport in porous media.

NUMERICAL SOLUTION

Since analytic solutions to the governing equations are unavailable except for special cases, numerical techniques must be employed. Harlan (1973) developed the first numerical computer model, using the finite difference method to solve the coupled water flow and heat transport equations for variably-saturated, variably-frozen soil derived on the basis of the mechanistic approach. Guymon and Luthin(1974)has solved similar equations using the finite element method.

Kung and Steenhuis (1986) used the finite difference method to solve the water flow and heat transport equations derived with the irreversible thermodynamics approach to simulate heat and water transfer in a variably-saturated, variably-frozen nonheaving soil.

Flerchinger (1987) used the finite difference method to solve the simultaneous heat and water equations given by equations (9) and (10), and the equations for a snowpack and residue layer. This effort resulted in the development of the SHAW model. The finite difference approximation to equations (9) and (10) can be written as the following equations respectively (see Flerchinger, 1987 for detail) for the discretized soil profile illustrated in Figure 1.

$$\left(\frac{\bar{\lambda}_{i-1}}{z_i - z_{i-1}} + \rho_w c_w \bar{q}_{i-1} + c_v \bar{q}_{vi-1}\right)\left[\omega\left(T_{i-1}^{j+1} - T_i^{j+1}\right) + (1-\omega)\left(T_{i-1}^{j} - T_i^{j}\right)\right]$$
$$-\left(\frac{\bar{\lambda}_{i}}{z_{i+1} - z_{i}} + \rho_w c_w \bar{q}_{wi} + c_v \bar{q}_{vi}\right)\left[\omega\left(T_{i}^{j+1} - T_{i+1}^{j+1}\right) + (1-\omega)\left(T_{i}^{j} - T_{i+1}^{j}\right)\right] + S_h \Delta z_i$$
$$= \frac{\Delta z_i}{\Delta t}\left[\left(\bar{C}_i + L_v \frac{\partial \rho_v}{\partial T}\right)\left(T_i^{j+1} - T_i^{j}\right) - \rho_i L_f\left(\theta_{i_i}^{j+1} - \theta_{i_i}^{j}\right)\right] + L\left(\bar{q}_{vi} - \bar{q}_{vi-1}\right) \tag{17}$$

$$\bar{k}_{i-1}\left[\frac{\omega\left(\psi_{mi-1}^{j+1} - \psi_{mi}^{j+1}\right) + (1-\omega)\left(\psi_{mi-1}^{j} - \psi_{i}^{j}\right)}{z_i - z_{i-1}} + 1\right]$$
$$-\bar{k}_{i}\left[\frac{\omega\left(\psi_{mi}^{j+1} - \psi_{mi+1}^{j+1}\right) + (1-\omega)\left(\psi_{mi}^{j} - \psi_{mi+1}^{j}\right)}{z_{i+1} - z_{i}} + 1\right] + S_{wi}\Delta z_i + \frac{\bar{q}_{vi-1} - \bar{q}_{vi}}{\rho_w}$$
$$= \frac{\Delta z_i}{\Delta t}\left[\theta_i^{j+1} - \theta_i^{j} + \frac{\rho_i}{\rho_w}\left(\theta_{i_i}^{j+1} - \theta_{i_i}^{j}\right)\right] \tag{18}$$

where subscripts i indicates space node, a bar over any variable denotes a time average quantity, and j indicates time, and ω is weighting factor.

Because of nonlinear nature of the coupled heat and water equation, the Newton-Raphson iterative technique was used for the solution.

THE SHAW MODEL

Because of model availability and its physical basis, the SHAW model was selected for testing with the measured field data in this study. The model requires 4 input data files.

One for the description of input and output data files. one for hourly weather data which includes air temperature, wind speed, relative humidity, solar radiation, and precipitation. One for soil temperature profile data (at least two profiles are required for the initial profile and for ending profile). One for soil water content profile (requirements similar to temperature profile), and one for soil site parameters including soil-snow-residual property data.

Output of the SHAW model gives 9 output files including: 1). General output information and hourly or daily temperature, moisture and solute profile; 2). Side by side predicted and measured moisture and temperature profiles; 3). Predicted temperature profiles; 4). Predicted moisture profiles; 5). Water balance summary; 6). Frost and ice content profile; 7). Summary of energy flux at the surface; 8). Total salt concentration profiles; and 9). Solute concentration of soil solution.

FIELD SITE DESCRIPTION

The site of the field testing data acquisition is located at the Rosemount Experiment Station in Rosemount, Minnesota. The slope of the land is essentially zero. The land was cultivated and the top 20 cm was considered as the tilled layer. There was no residue cover on the soil surface during the period of data acquisition. A plan view of the experiment site is illustrated in Figure 2. A weather station at the site measured incoming solar radiation, precipitation, air temperature, relative humidity, and wind speed. The sensors for measuring temperature and water content were installed in the soil profile as shown in Figure 3. Total water content was measured with the neutron scattering method, while liquid water content was measured with the method of time domain reflectometry. Soil temperature was measured with thermocouples.

Soil Parameters

Measured soil data included soil texture and bulk density at several depths in the soil profile. The measured bulk density and soil texture data are presented in Table 1.

The total porosity of the soil was estimated by assuming a particle density of 2.65 gm/cm^3. The soil hydraulic parameters including pore size distribution index b, air entry potential ψ_e, and saturated hydraulic conductivity K_s were estimated from soil bulk density and soil texture. Campbell (1985) presented empirical equations for calculating b, ψ_e, and K_s based on the geometric mean particle size, d_g (mm), and geometric standard deviation, σ_g (mm). These geometric properties can be calculated from the following equations.

$$d_g = \exp(x) \tag{23}$$

and $$\sigma_g = \exp(y) \tag{24}$$

where $$x = m_c \ln(0.001) + m_{si} \ln(0.026) + m_{sa} \ln(1.025) \tag{25}$$

$$y = \left[m_c(\ln 0.001)^2 + m_{si}(\ln 0.026)^2 + m_{sa}(\ln 1.025)^2 - x^2\right]^{1/2} \tag{26}$$

here m_c, m_{si} and m_{sa} are the mass fractions of clay, silt and sand.

Then b can be calculated from the equation (Campbell, 1985),

$$b = -2\psi_{es} + 0.2\sigma_g \tag{27}$$

where $$\psi_{es} = -0.5 d_g^{-1/2} \tag{28}$$

Flerchinger (1987) used the same procedure to calculate b for the SHAW model input. However, the constant -0.5 in equation was not used. Instead he used -0.2 because of a better fit to measured values of hydraulic properties. For this study, the two different coefficients were used to estimate two sets of input data. The equations from Campbell (1985) for ψ_e and K are related to b, which can be written in the form (Flerchinger, 1987),

$$\psi_e = \frac{\psi_{es}}{g}\left(\frac{\rho_b}{1.3}\right)^{0.67b} \tag{29}$$

$$K_s = 14.4\left(\frac{1.3}{\rho_b}\right)^{1.3b} \exp(-6.9m_c - 3.7m_{si}) \tag{30}$$

where $\psi_e =$ air entery value, m;

$\rho_b =$ bulk density, g/cm^3;

$g =$ the acceleration of gravity, $9.8\ m/sec^2$

$K_s =$ saturated hydraulic conductivity, cm / hr.

Based on the above equations, the soil parameters for hydraulic properties were calculated and are presented in Table 1. This table includes two sets of parameters for pore size distribution, air entry potential, and saturated hydraulic conductivity. One set was calculated from equation (28), which has a coefficient of -0.5. The other set was calculated from the same equation but with a coefficient of -0.2, which was used by Flerchinger (1987). Both sets of soil parameters were used for the soil tested in this study.

The thermal conductivity of soil is evaluated by the de Vries(1963) equation in the SHAW model. The equation can written as,

$$\lambda = \frac{\sum m_j \lambda_j V_j}{\sum m_j \lambda_j} \qquad (31)$$

where m_j, λ_j, and V_j are shape factor, thermal conductivity, and volumetric fraction of the j^{th} soil constituent, i.e. soil minerals, water, air, and ice.

For the thermal conductivity of soil mineral, the value of 7.5 was taken based on a weighted average of approximately 78% quartz (sand and silt) and 22% clay minerals with conductivity of 8.8 and 2.9 W/m-C respectively. The thermal conductivity of water, ice, and air were taken as 0.57, 2.2, and 0.025 W/m-C respectively (Hillel, 1980). The shape factors were determined as 0.20 for soil solid, 1.0 for water, 0.51 for ice, and 1.47 for air based on de Vries (1963) by assuming spherical granules. Flerchinger (1987) used 0.2 for soil solid, 1.0 for water, 0.5 for ice, and 2.5 for air based on measured field data. The only significant difference is the shape factor for air. However, because of the very small thermal conductivity of air, the difference in the shape factor of air should not make much difference in calculating thermal conductivity of the soil.

RESULTS AND DISCUSSION

The primary interest of the model testing is mainly on water and heat transfer. Therefore, salt transport in the soil is not considered although the SHAW model has the facility to predict salt transport. The simulation starts at the date of 11/5/89 and ends on 3/31/90. The measured initial water content and temperature profile is plotted in Figure 4. The lower boundary condition at 1 meter depth for temperature and water content is plotted in Figure 5.

Besides the two runs that were based on the calculated soil parameters, several other runs were made by varying the input soil parameters to assess the sensitivity of the predicted variables to the input parameters. The parameters tested were pore size distribution index, air entry potential, saturated hydraulic conductivity, shape factors for calculating thermal conductivity, and number of input soil temperature/water content profiles, and lower boundary temperature. The results of the run using the Flerchinger coefficient are plotted in this paper because it yielded results in better agreement with the field data than the run using the Campbell coefficient.

Temperature Profile

The predicted soil temperature at depths of 10, 20, 40, 80, and 100 cm are plotted with the measured soil temperature in Figures 6 to 10.

For the soil at 10 cm, the comparison of measured and predicted field temperature can be seen in Figure 6. It shows that the predicted temperature agrees well with measured temperature. The lowest temperature is about -14 °C for both measured and predicted which occurs at day 351 and 356, respectively. The predicted minimum temperature occurs five days earlier than the measured temperature. Before the soil temperature gets to the lowest point, for a period of about 10 days the predicted temperature almost exactly fits to the measured temperature. This happens around day 337. Before and after this period, the predicted temperature is lower than the measured temperature for some days. It seems that the predicted temperature is more responsive to the cold weather. The two downward peaks of the predicted temperature at about day 320 indicates that the soil at 10 cm is frozen. The measured data shows that the soil is just at the freezing point. After the 10 cm depth reached its minimum temperature, the predicted temperature agreed quite well with the measured temperature for the rest simulation period.

Figure 7 shows the predicted and measured temperature for the 20 cm depth soil. It can be seen that the overall trend of the temperature variation at 20 cm depth is similar to 10 cm depth. However, the curves for both predicted and measured temperature have been smoothed and the magnitude of the peaks observed at the 10 cm depth has been reduced at the 20 cm depth. The lowest predicted and measured temperature was about -12.5 °C, which occurs about 2 days later than at the 10 cm depth. For the days after the lowest point the predicted temperature and the measured temperature are in good agreement

The same is true for 40 cm depth compared to the shallower depths of 10 and 20 cm. It can be seen from Figure 8 that both the predicted and measured temperature curves are smoother and have a reduced peak amplitude. Generally speaking, the predicted temperature fits the measured temperature very well.

The predicted and measured temperatures for 80 cm depth can be seen from Figure 9. Both the curves of the predicted and measured temperatures become quite smooth here. The single low temperature point from the measured temperature appears at day 365. This may be considered as an error in the temperature measurement. The lowest predicted and measured temperature is about - 2.8 °C. The overall agreement between measured and observed values is still very good.

Flerchinger (1987) simulated soil temperature at the surface, 7.5 and 15 cm depth, for a conventionally-tilled bare soil surface, and a no-till plot with heavy residue cover. The results showed that the predicted soil temperature for all those depths agreed very well with the measured temperatures. The results presented from this study confirm the results given by Flerchinger (1987) and demonstrate that the SHAW model has a good capability for predicting soil temperature profiles.

Water Content Profile

The model output results give the total water content and ice content. For comparison with the measured liquid water content data, the predicted liquid water content were obtained by subtracting the predicted ice content from the predicted total water content. The predicted liquid water content at depths of 10, 20, 40, 80, and 100 cm are plotted with measured field data in Figures 10 to 14.

For the liquid water content at 10 cm depth, Figure 10 shows that the predicted liquid water content does not agree well with the measured field data, especially in the early winter when the soil is freezing. The predicted liquid water content is much lower than measured for much of the simulation period although the variations in liquid water content have similar patterns. The time of thawing observed is very similar to the predicted time of thawing at the 10 cm depth

Similar to the results for the 10 cm depth, Figure 11 shows that the predicted liquid water content of the 20 cm depth soil is generally lower than the measured liquid water content. From Figure 11, it can be clearly seen that the predicted liquid water content suddenly drops around day 320, while the sudden drop happens for measured data around day 337. The thawing for both predicted and measured happens about the same time at day 435. A significant difference between measured and predicted liquid water content is also observed after day 435, where the temperature is above 0 °C. Since at this point all the water in the soil at 20 cm is liquid water, this result indicates that the total water contents of the predicted and measured are not in good agreement.

For the 40 cm depth, the predicted liquid water content does not agree well with measured data (Figure 12). Although the predicted freezing time and measured freezing time agree well, the predicted liquid water content dropped to a lower level after freezing. Even larger differences can be seen for the predicted and measured liquid water content after day 435. The measured data indicate that the rate of thawing at the 40 cm depth is much faster than the predicted rate of thawing.

Figure 13 shows the predicted and measured liquid water content at 80 cm. The predicted liquid water content agrees with the measured in certain period of time. The first significant difference is observed during the period from day 320 to day 350. During that time the predicted liquid water content is increasing while the measured water content remains fairly constant. The predicted time of first freezing of the water at the 80 cm depth occurs at about the same time as the measured time. After the liquid water content dropped to the same lowest point at around day 360, the measured liquid water content suddenly increased a significant amount while the predicted liquid water content increased a lesser amount. A large difference is also observed for the period after day 432. The measured data indicates the soil thawed very fast from a liquid water conent of 0.075 to 0.19, while the predicted liquid water content increases gradually. The reason for the measured liquid water content suddenly dropped after the day 442 is not immediately clear because there is no temperature drop at this point. However, drainage of water from this depth may account for this change in liquid water content.

For the 100 cm depth it can be seen from Figure 14 that the predicted liquid water content agrees well with measured data before day 355. After that the measured liquid water content continuously dropped to about 0.03 and a sudden increase is observed at about day 435. This indicates that the soil was frozen at the 100 cmd depth. The predicted results indicate that the soil was not frozen even though the temperature was below 0 °C.

From the figures of liquid water content, it was found that the predicted water content profile does not agree well with measured data. The reasons may come from improper soil parameters, errors in the measurement of liquid/total water content, underestimating the initial water content profile, or model limitations. An attempt has been made to improve the prediction for water content profile by varying parameters including pore size distribution index, saturated hydraulic conductivity, and air-empty potential. However, no significant improvements have been observed from this effort.

Flerchinger (1987) compared the total water content predicted with the SHAW model to measured data total water content data for a soil profile up to a 170 cm depth. The comparisons were made for selected days, not for the entire period as we have done here.

For those selected day it was observed that most of the predicted total water content profiles agree well with the measured data. However, significant differences between predicted and measured total water contents were also found on some of the selected days.

Frost and Thaw Depth

The predicted frost and thaw depth are plotted with observed data in Figure 15. Because we had no data for direct measurement of frost and thaw depth, the actual frost and thaw depth were estimated from the measured liquid water content and temperature profile data. The soil was considered frozen at a given depth when the temperature at that depth fell below 0 °C and the liquid water content at that depth showed a sudden drop. An exact measure of the maximum depth of frost penetration could not be made because the temperature and water content sensors were not closely spaced, and only existed down to 1 meter depth. Based on this field data it is estimated that the maximum frost depth over the entire winter period was about 1 meter. The predicted maximum depth is about 54 cm for run 1 and 92 cm for run 2. This is the main reason that the results of run 2 were used in the previous presentation.

The comparison of predicted and measured frost and thaw depth can be seen from Figure 15. It was found that the predicted frost depth agrees very well with measured data before day 360 except at the 20 cm depth. The predicted frost depth advanced faster from the 10 cm depth to the 30 cm depth when compared to the measured field data. On day 360, both the predicted and the measured frost depth reached the maximum value. However, the predicted maximum frost depth is about 5 cm less than the measured maximum frost depth.

The predicted thawing started from day 430, which is about the same time as the initiation of thawing estimated from the measured data. Because of the alternation between the cold and warm weather, there are several thaw and freezing cycle. The measured data shows that the whole soil profile thawed completely on day 455. However, the model prediction showed that total thaw occurred about 4 days later.

Flerchinger (1987) simulated the frost depth for 6 different plots with different tillage or different surface cover conditions. The results were compared to the frost depth estimated by electrical resistance block and frost tube methods. The predicted frost depths were gernerally midway between the frost depths estimated by the resistance block and frost tube data. This indicated a reasonable agreement between predicted and measured frost depth. However, for 2 of tested plots, the predicted results slightly overpredicted frost depth.

Flerchinger and Hanson(1989) applied the SHAW model to a rangeland watershed. The simulation was performed for three sites through the 1986-1987 winter, and one site through a two winter period of 1985-1987. The results show very good agreement between predicted temperature and measured temperature at the depth of 2.5, 5, and 10 cm. The predicted maximum frost depth generally agreed with measured value within less than a 10% error. For one site a 14% difference between the predicted and measured maximum frost depth was found. The authors did not show water content prediction results in this paper.

Lundin (1989) reported simulation results from the SOIL model which were similar to the results presented in this paper. Very good agreement was found between predicted and measured soil temperatures at 5, 20, and 40 cm depths. Agreement between predicted and measured liquid water contents were somewhat better than that presented in this paper.

Pikul and Zuzel (1990) presented predicted total water content and temperature in the top 1 cm of a soil profile with a bare surface for a 20 hour period, and compared the predictions to measured data. Good agreement was found between the predicted and measured values.

SUMMARY AND CONCLUSION

The SHAW model has been tested with measured soil liquid water content and temperature data acquired over the winter of 1989 for a field site located at Rosemount Minnesota. Very good agreement was observed between the predicted and measured soil temperature profiles, and quite good agreement was found between the frost depth estimated from the field data and the frost depth predicted by the model. Because thaw depth measurements were less reliable than frost depth measurements it is difficult to evaluate the accuracy of the thaw depth predictions produced by the SHAW model. However, the SHAW model did predict the initiation of the thaw quite well.

In the present study the liquid water content profile measured with the method of time domain reflectometry was not predicted satisfactorily by the SHAW model. A number of reasons can be formulated for this unsatisfactory result. We feel that the primary reason is that the liquid water retention characteristics of the soil were not measured directly for freezing conditions, but were instead derived from estimates using equations based on grain size distribution and bulk density of the soil. It is unlikely that the unsatisfactory result can be attributed to limitations of the mathematical equations upon which the SHAW model is based. However, this possible source of inaccuracy will be assessed in future studies.

Other researchers have demonstrated similar ability to simulate quite accurately the observed temperature profiles in a soil subjected to freezing/thawing cycles. At this point there still remains the problem of accurately simulating the liquid and total water content in a soil profile subjected to freezing and thawing processes. In none of the work we have reviewed has this problem been satisfactorily addressed. A major reason for this probably lies in the inadquate definition of the hydraulic properties of variably-saturated, variably-frozen soils. Additional future work will be needed to better characterize these hydraulic properties before this issue can be adequately addressed.

The SHAW model was originally intended to solve water flow and heat transport problems for conditions commonly found in agricultural, forested, and range lands. These conditions typically have a soil surface covered with vegetation/residue in addition to snow. Because of its flexibility it will be possible to apply this model to paved soil conditions after some modifications to account for the pavement being the upper boundary for the soil

Although the SHAW mdoel requires many input parameters and variables to describe weather, soil, and surface cover conditions, it has the potential to be a useful tool to evaluate the fate of water beneath pavements.

REFERENCES

Berg, R. L., G. L. Guymon and T. C. Johnson, Mathematical model to correlate frost heave of pavements with laboratory predictions, U.S.Army Cold Reg. Res. Engg. Lab. Rep. 80-110, Hanover, NH, 54 pp., 1980.

Campbell, D. S., Soil physics with basic: Transport models for soil-plant system. Elsevier Soil Publishing Co. Amsterdam. 150 pp., 1985.

de Vries, D. A., Thermal properties of soils, Chapter 7 in Physics of Plant Environment. W. R. van Wijk (Eds) North-Holland Publishing Co., Amsterdam., 1963.

Flerchinger, G. N. and K. E. Saxton, Simultaneous heat and water model of a freezing snow-residure-soil system, 1. Theory and development. Transaction of the ASAE, vol. 32(2)., 1989.

Flerchinger, G. N., Simultaneous heat and water model of a snow-residure-soil system, Ph.D. Dissertation, Washington state university, 1987.

Flerchinger, G.N. and C.L. Hanson, Modeling soil freezing and thawing on a rangeland watershed, Transactions of the ASAE, vol.32(5): 1551-1554, 1990.

Groenevelt P. H. and Kay, B. D., On the interact of water and heat transport in frozen and unfrozen soils: II. The liquid phase. Soil Sci. Soc. Amer. Proc., vol. 38, 1974.

Guymon, G. L. and J. L. Luthin, A coupled heat and moisture transportmodel for arctic soils, Water Resour. Res. 10:995-1001, (1974).

Harlan, R. L., Analysis of coupled heat-fluid transport in partially frozen soil., American Geophysical Union., 1973.

Hillel, D., Fundamentals of soil physics, Academic press., 1980.

Hoekstra, P., Moisture movement in soils under temperature gradients with the cold side temperature below freezing, Water Resour. Res. 2:241-250, 1966.

Jumikis, A. R., Some concepts pertaining to freezing soil systems, Water and Its Conduction in Soils, Spec. Rep. 40, pp. 178-190, edited by H. F. Winkerhorn, Highway Res. Board, Washington, D. C., 1958.

Jury, W. A., Simultaneous transport of heat and moisture through a medium sand., Ph. D. Thesis, University of Wisconsin, Madison, 1973.

Kay, B. D. and P. H. Groenevelt, On the interact of water and heat transport in frozen and unfrozen soils: I. basic theory; the vapor phase. Soil Sci. Soc. Amer. Proc., vol. 38, 1974.

Kay, B. D. and Perfect E., State of the art: Heat and mass transfer in freezing soils, 5th international symposium on ground freezing, Balkema, Rotterdam, 1988.

Kung, S. K. J. and T. S. Steenhuis, Heat and moisture transfer in a partly frozen nonheaving soil. Soil Sci Soc. Am. J., vol. 50:1114-1122, 1986.

Lundin, L.-C., Water and heat flows in frozen soils, basic theory and operational modeling, Doctoral dissertation at Uppsala University, 1989.

Miller, R. D., Freezing phenomena in soils, in Applications of Soil Physics(Hillel, 1980), 1980.

Palmer, A. C., Ice lensing, thermal diffusion and water migration in freezing soils, J. Glaciol., 6, 681-694, 1967.

Philip, J. R. and D. A. de Vries, Moisture movement in porous materials under temperature gradients. Transactions, American Geophysical Union, 1957.

Pikul, J.L.,Jr. and R.R. Allmaras, A field comparison of null-aligned and mechanistic soil heat flux, Soil Sci. Soc. Am. vol.48: 1207-1214, 1986

Pikul, J.L.Jr. and J.F. Zuzel, Heat and water flux in a diurnally freezing and thawing soil, Frozen Soil Symposium, Spokane, Washington, 1990.

Taylor, S.A. and J.W. Cary, Linear equations for simultaneous flow of matter and energy in a continuous soil system, Soil Soi. Soc. Am. Proc. 28:167-172.(1964).

Wallace, A. I. and P. J. Williams, Problems of building roads in the north, Can. Geographical J. 89(1-2):40-47, 1974.

List of figures:

List of tables.

Xia Xu et al. Figure 1.

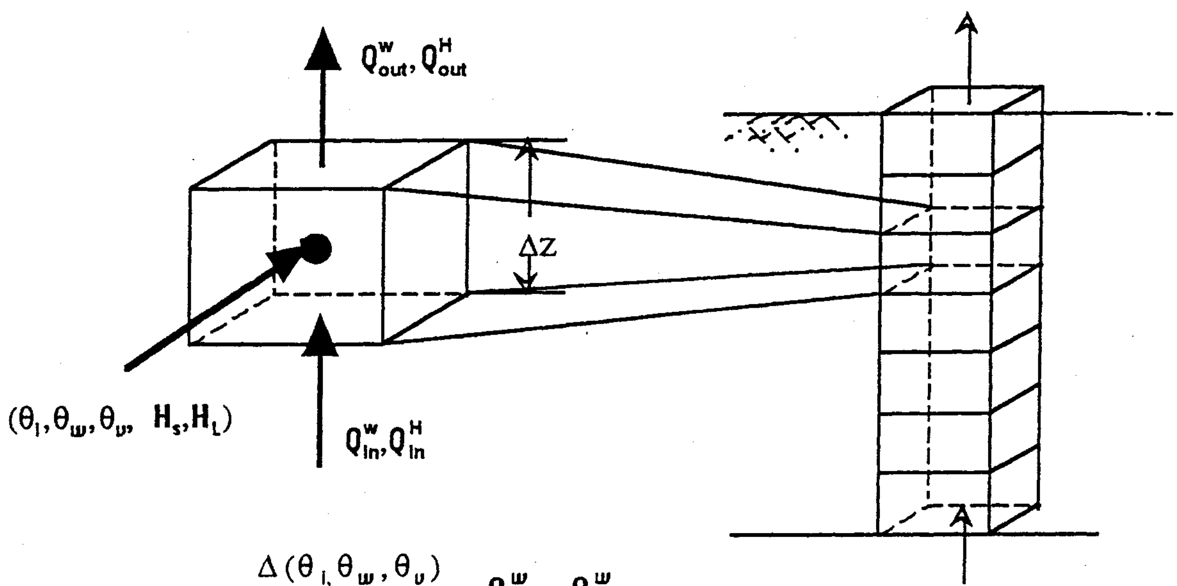

WATER $$\frac{\Delta(\theta_l, \theta_w, \theta_v)}{\Delta t} = Q^w_{in} - Q^w_{out}$$

HEAT $$\frac{\Delta(H_s, H_L)}{\Delta t} = Q^H_{in} - Q^H_{out}$$

Xia Xu et al. Figure 2.

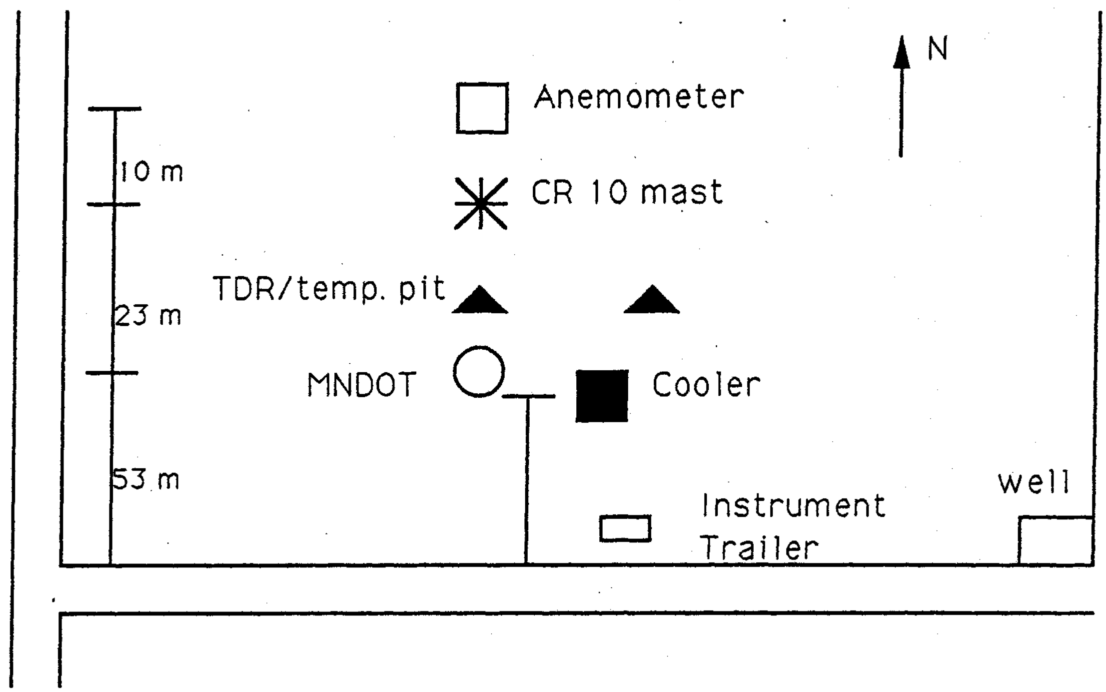

Xia Xu et al. Figure 3.

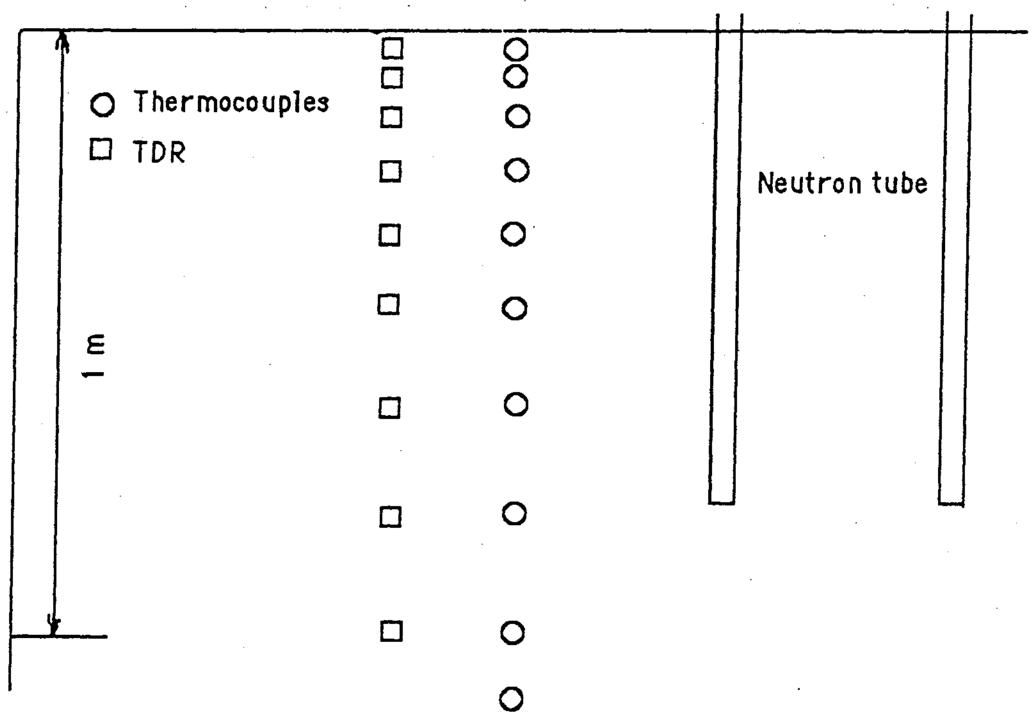

Xia Xu et al. Figure 4.

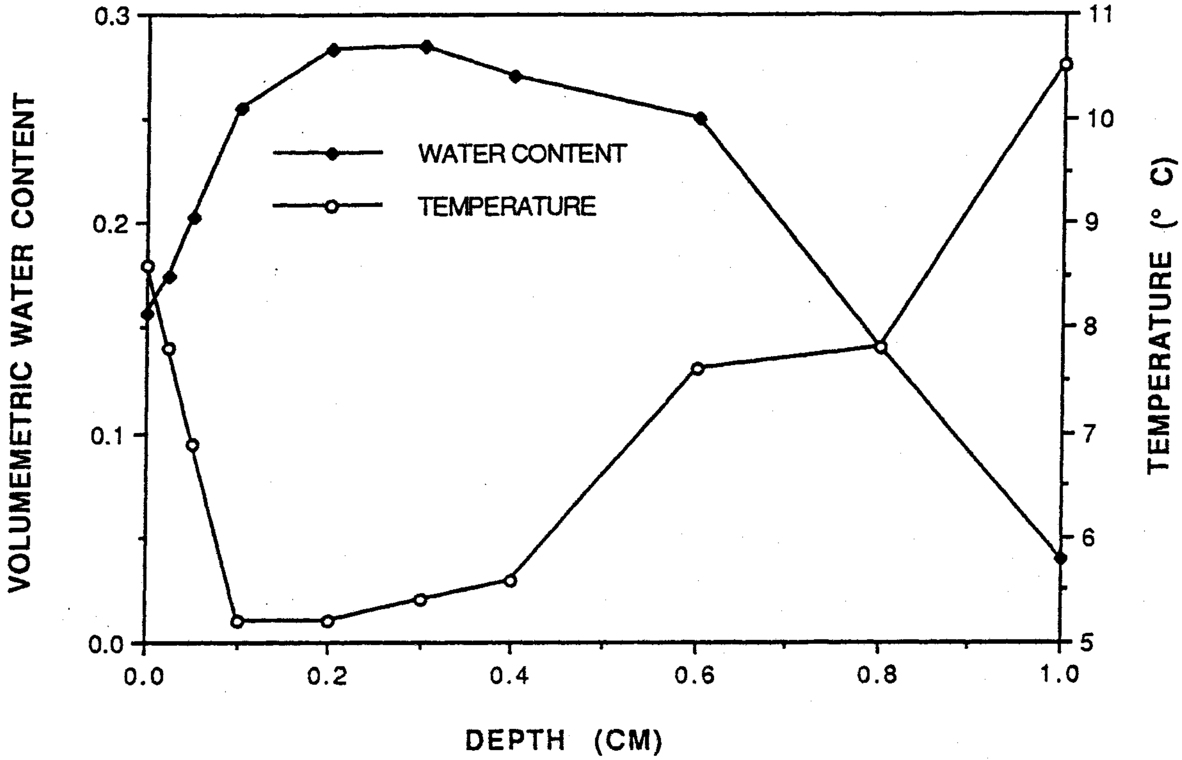

Xia Xu et al. Figure 5.

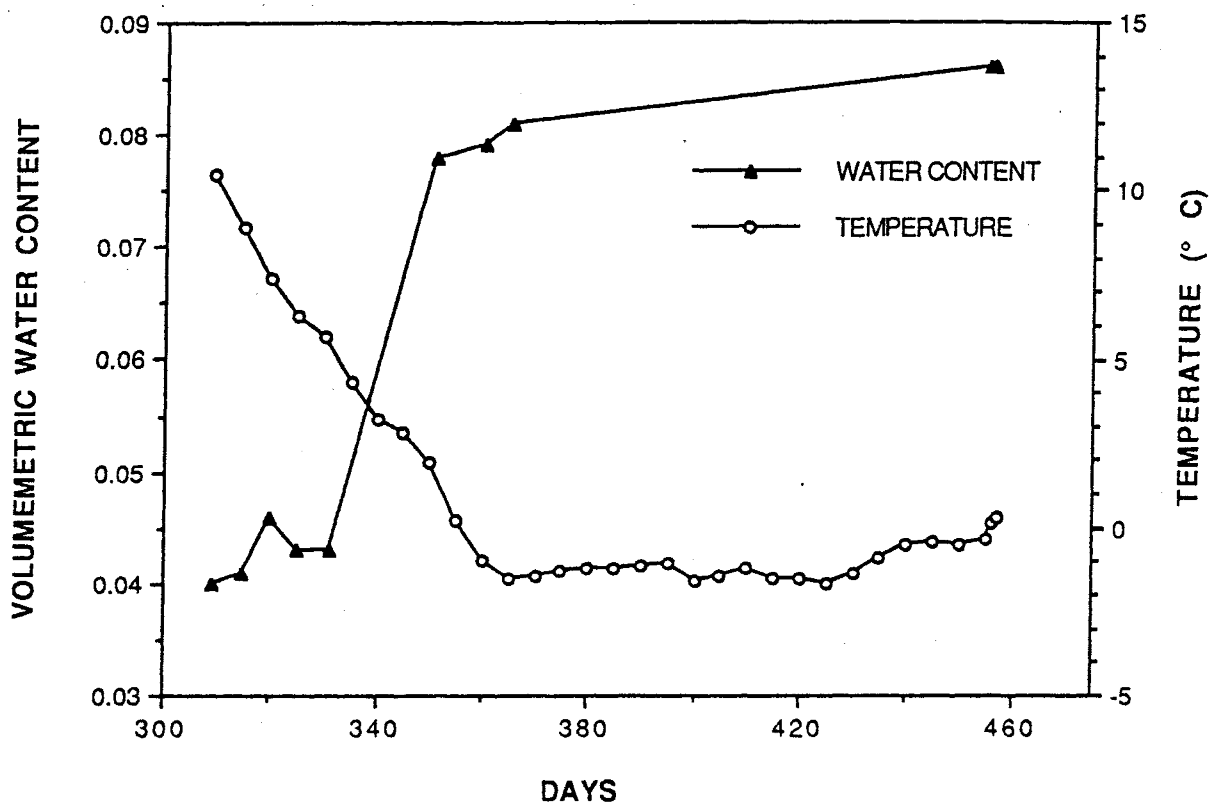

Xia Xu et al. Figure 6.

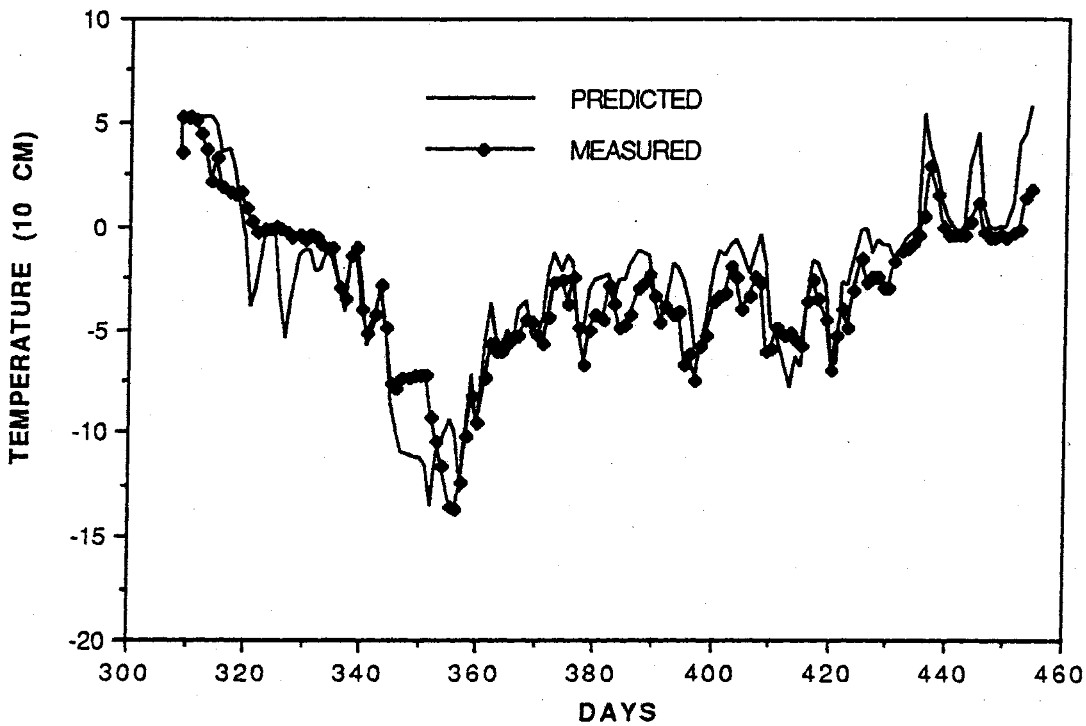

Xia Xu et al. Figure 7.

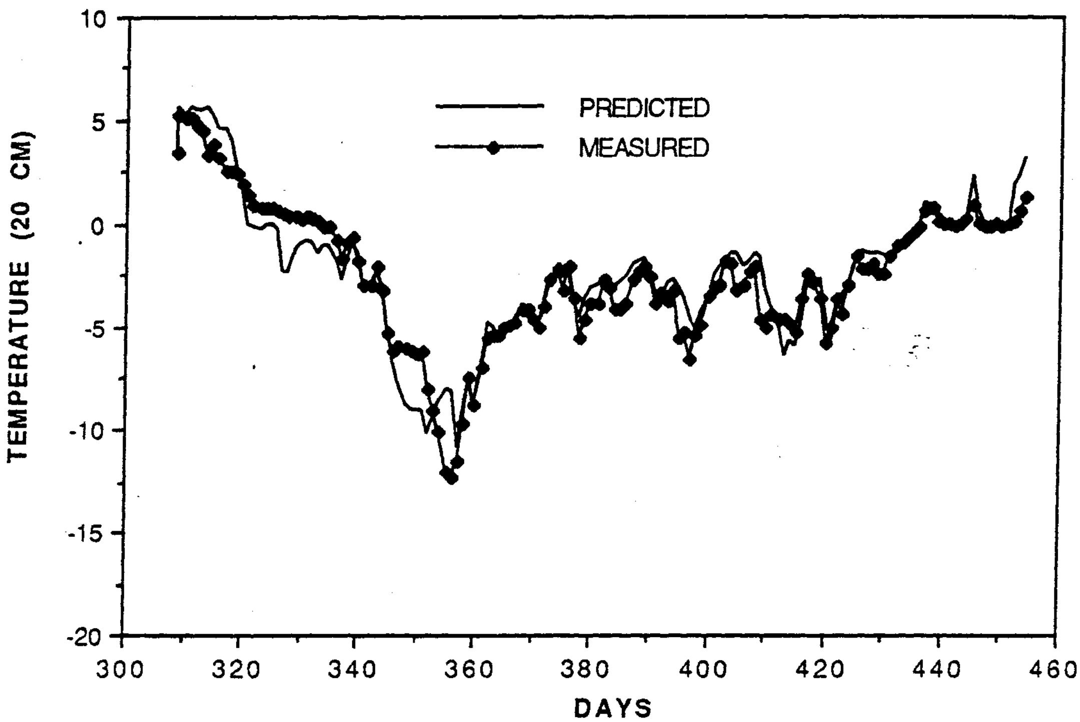

Xia Xu et al. Figure 8.

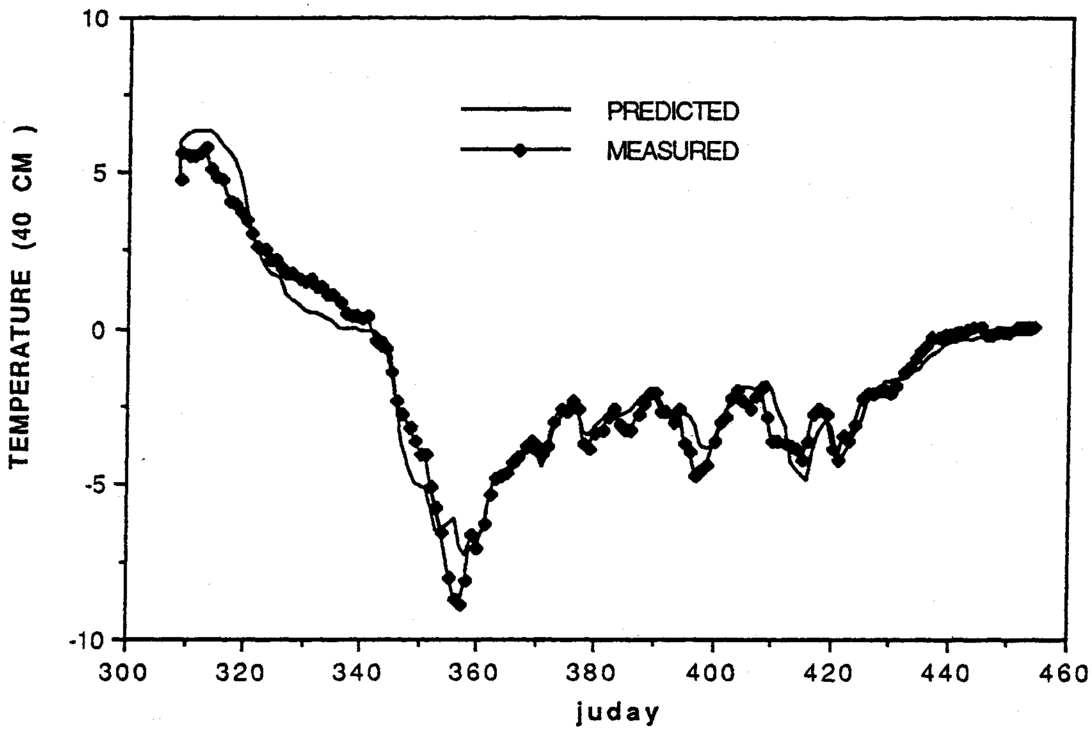

Xia Xu et al. Figure 9.

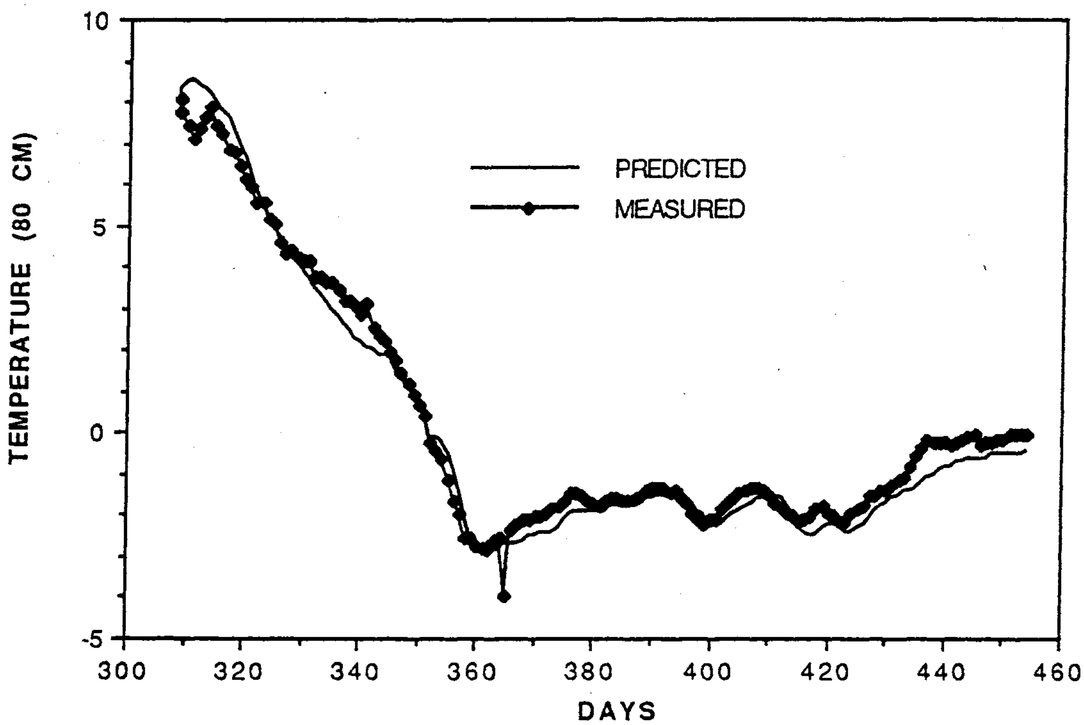

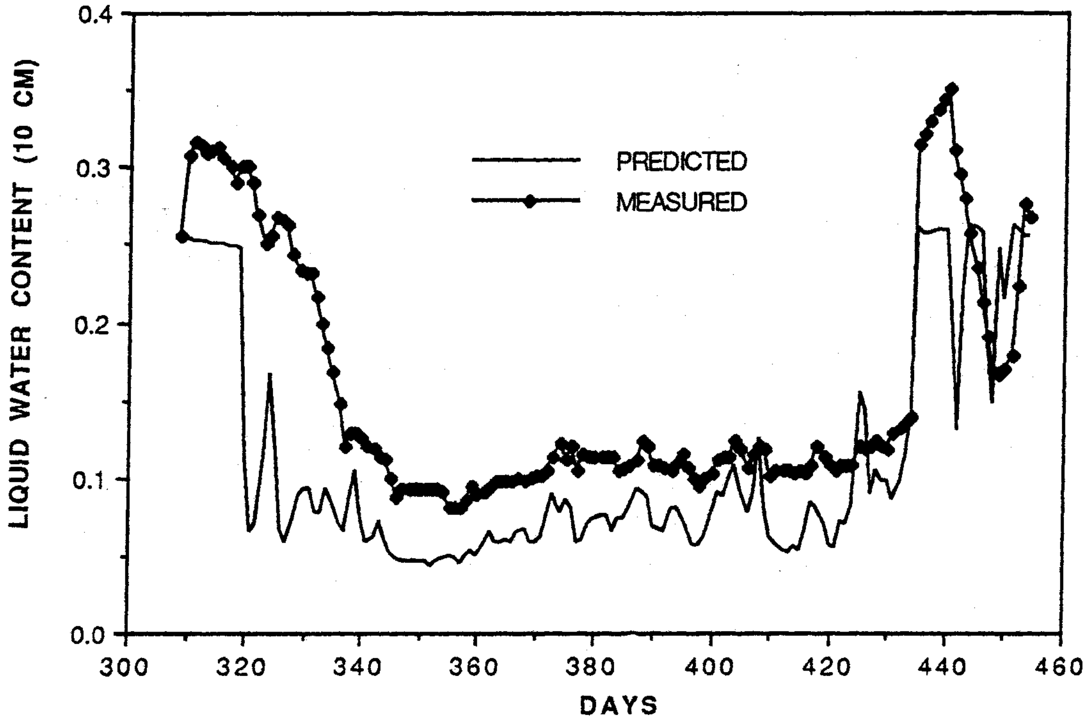
LIQUID WATER CONTENT (10 CM)
0.0
0.1
0.2
0.3
0.4
300
320
340
360
380
400
420
440
460
DAYS
PREDICTED
MEASURED

Xia Xu et al. Figure 11.

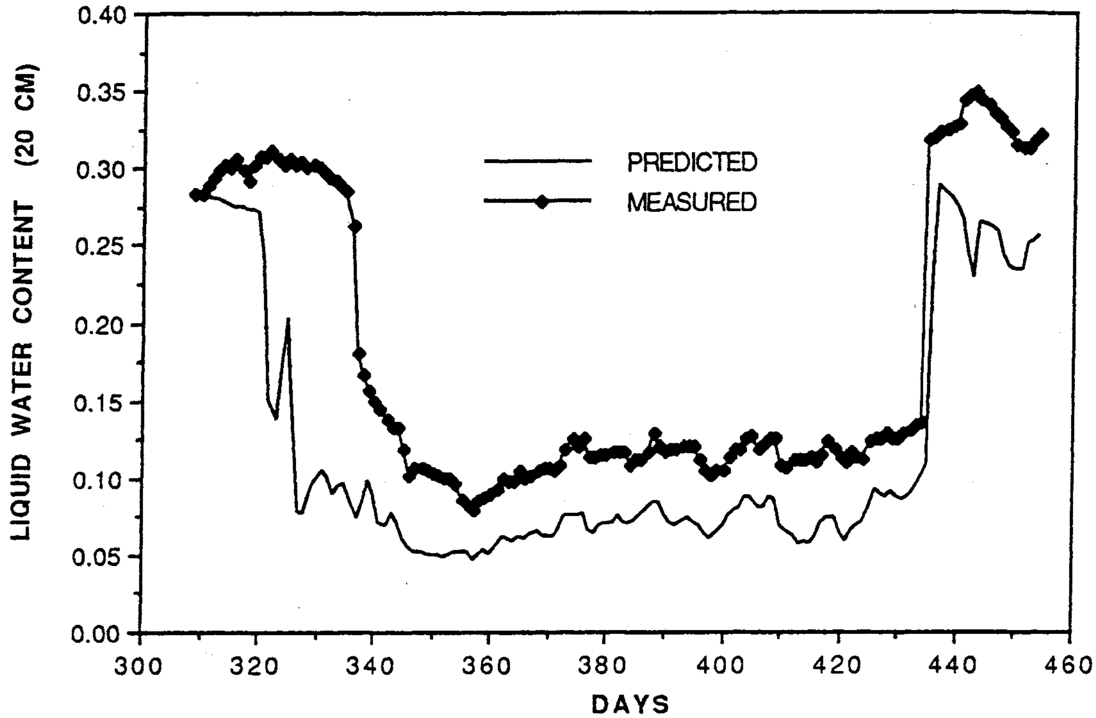

Xia Xu et al. Figure 12.

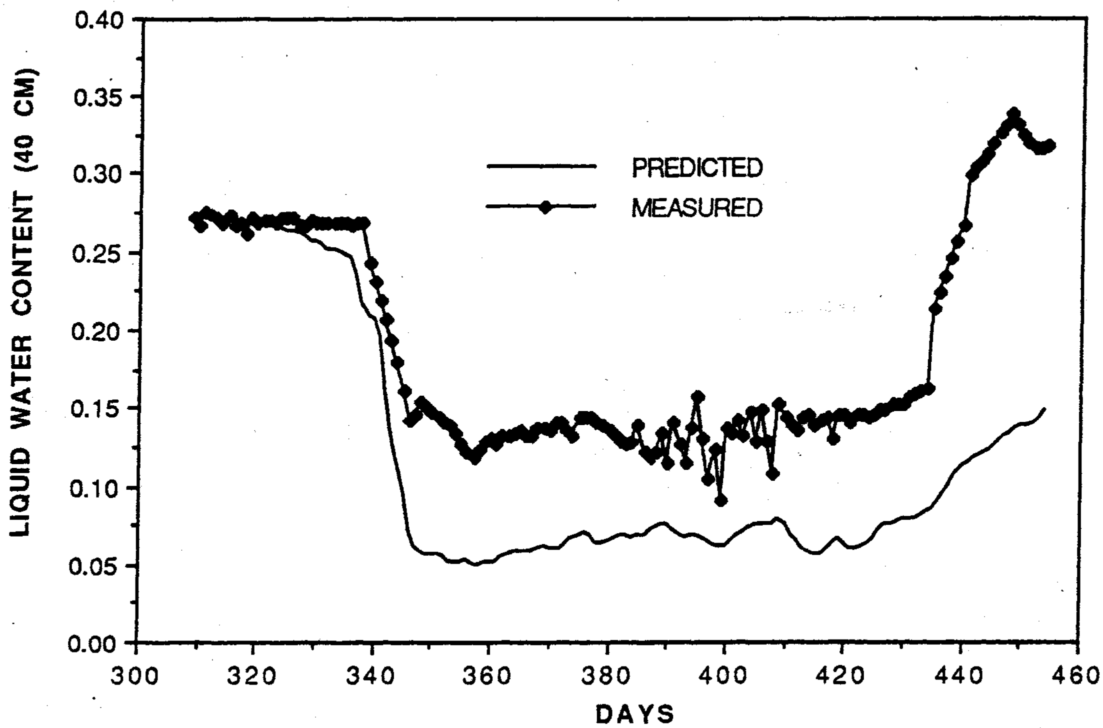

Xia Xu et al. Figure 13.

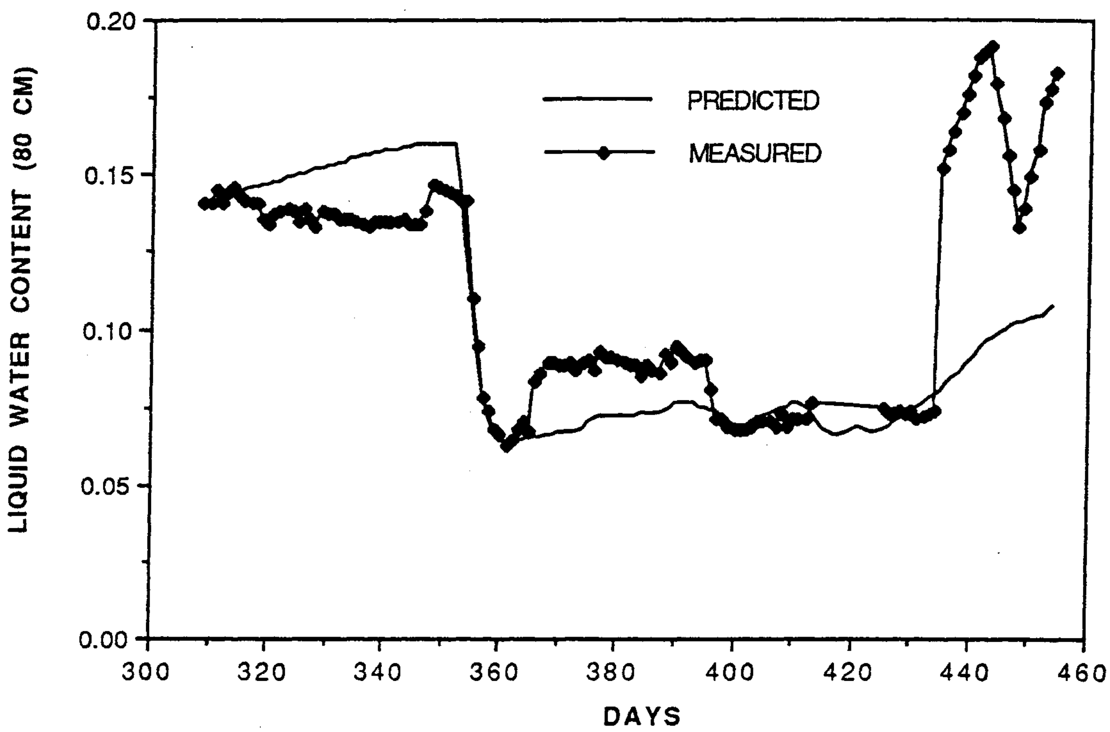

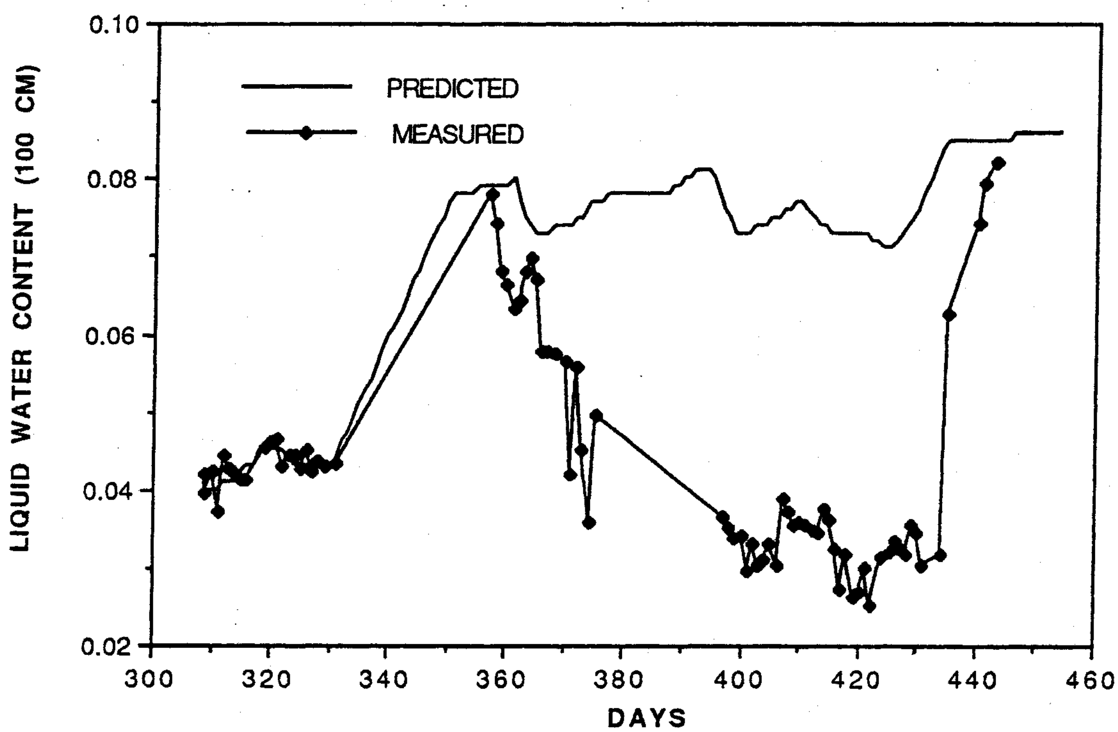
PREDICTED
MEASURED
LIQUID WATER CONTENT (100 CM)
0.10
0.08
0.06
0.04
0.02
300
320
340
360
380
400
420
440
460
DAYS

Xia Xu et al. Figure 15.

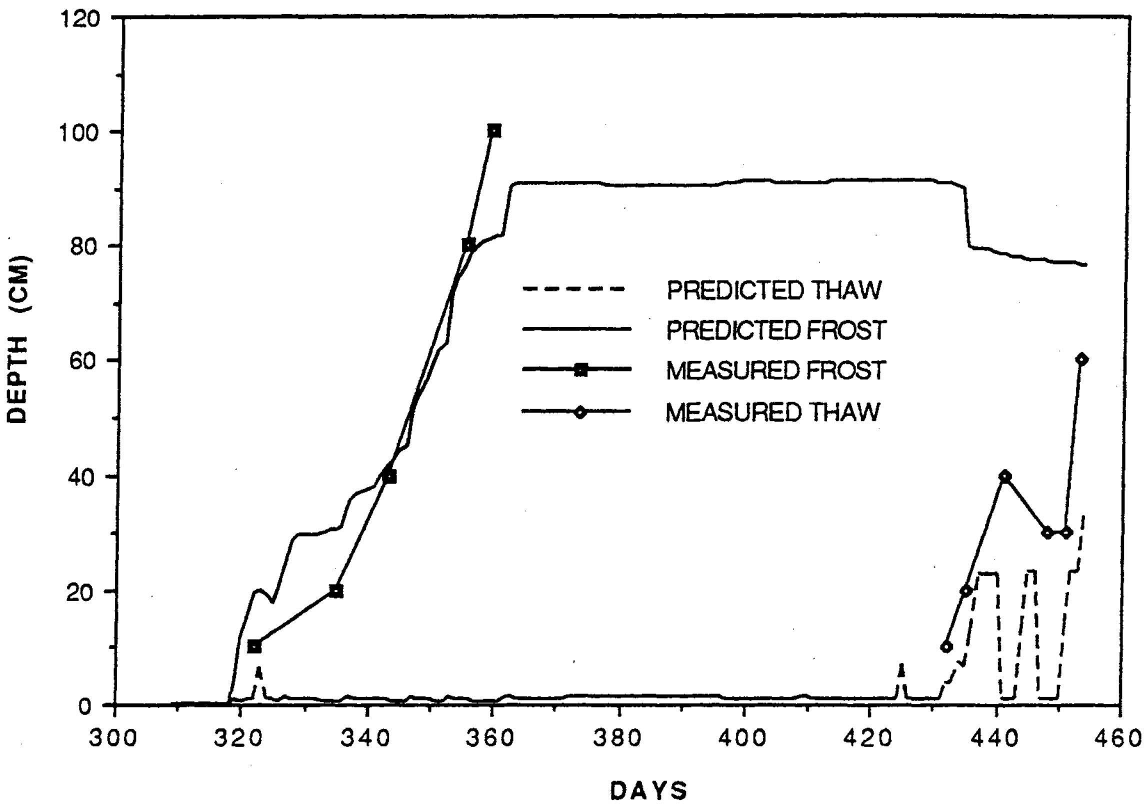

Depth (cm)	BD (g/cm³)	Sand	Silt	Clay	b*	MPe* (cm)	Ks* (cm/h)	b#	MPe# (cm)	Ks# (cm/hr)
2.5	1.016	0.19	0.58	0.23	8.24	-8	4.82	4.42	-6	1.42
5.0	1.012	0.19	0.58	0.23	8.24	-8	5.03	4.42	-6	1.45
10.0	1.112	0.19	0.58	0.23	8.24	-14	1.83	4.42	-8	0.84
20.0	1.204	0.19	0.58	0.24	8.44	-22	0.75	4.49	-11	0.50
30.0	1.270	0.15	0.64	0.22	8.41	-31	0.38	4.29	-13	0.34
40.0	1.261	0.15	0.64	0.22	8.41	-29	0.41	4.29	-13	0.35
60.0	1.275	0.19	0.59	0.22	8.09	-29	0.44	4.33	-12	0.40
80.0	1.345	0.31	0.50	0.19	7.07	-29	0.45	4.20	-11	0.51
100.0	1.536	0.25	0.57	0.18	7.20	-60	0.11	4.05	-17	0.21

* Calculation was based on Campbell constant, -0.5, in equation (28).

Calculation was based on Flerchinger constant, -0.2, in equation (28).